OPTICAL WIRELESS COMMUNICATIONS SYSTEM FOR SECURE INFORMATION EXCHANGE

An Undergraduate Research Scholars Thesis

by

CHAANCE T. GRAVES

Submitted to the Undergraduate Research Scholars program at
Texas A&M University
in partial fulfillment of the requirements for the designation as an

UNDERGRADUATE RESEARCH SCHOLAR

Approved by Research Advisor: Dr. Christi Madsen

May 2017

Major: Electrical Engineering

TABLE OF CONTENTS

ABSTRACT

Optical Wireless Communications System for secure information exchange

Chaance T. Graves
Department of Electrical and Computer Engineering
Texas A&M University

Research Advisor: Dr. Christi Madsen
Department of Electrical and Computer Engineering
Texas A&M University

Currently in our society, many of the devices we use in our daily lives operate within the restricted and crowded Radio Frequency (RF) bandwidths. Overcoming this challenge presents a unique opportunity to utilize the free space optical standard further into future technologies such as Internet of Things (IoT) networks. Furthermore, we examined the design parameters, compared the uses of optical communication to current market 2.4 GHz Radio Frequency (RF) solutions with the emphasis directed to the physical layer security of the data link. An overview of the prototype system describes the design and characterizations of an indoor free space optical system comprised of both a transmitter and receiver circuit. Additional simulations and experimental results show a proof of concept of system reliability for applications such as Wireless Local Area Networks (WLANs) along with benchmarks such as high-speed data transmission bit rate over the span of various distances of the free space channel.

LIST OF KEY ABBREVIATIONS

OWC	Optical Wireless Communication
FSO	Free Space Optics
RF	Radio Frequency
OOK	On Off Keying
VLS	Visible Light Spectrum
EMI	Electromagnetic Interference
TX	Transmitter
RX	Receiver
IoT	Internet of Things
WLAN	Wireless Local Area Network
LED	Light Emitting Diode
LD	Laser Diode
APD	Avalanche Photodiode
POF	Plastic Optical Fiber
PMMA	Poly-Methyl-Methacrylate
LOS	Line of Sight
FOV	Field of View
NA	Numerical Aperture
SNR	Signal-to-Noise Ratio
BER	Bit Error Rate
UWB	Ultra-wideband

IM/DD	Intensity Modulation/Direct Detection

SECTION I

INTRODUCTION

Currently in our society, many of the devices we use in our daily lives operate within the restricted and crowded Radio Frequency (RF) bandwidths [9]. Overcoming this challenge presents a unique opportunity to utilize the free space optical standard. Specifically, the objectives of the optical wireless communications (OWC) system is to define specific benchmarks and requirements in order to design and test a proof of concept experimental testbed. The following accomplishments are to: achieve a data rate greater 100 Mbps for a distance of 1 meter, understand the basic physics of optics, identify methods for secure communications and low power consumption, and to be able to hide the modulated signal in ambient noise.

Information can be formatted and modulated as either analog or digital carrier waves. The key advantages of transmitting information via digital communication provide ease of use for error correction and modulating optical light sources efficiently [7]. Optical wireless communication systems possess the capability of being integrated within future Internet-of-Things (IoT) devices and in other sorts of emerging connected devices. Additionally, OWC systems can be utilized for current market solutions such as HDTV, computer networks, high speed Internet access, complementary to Fiber-to-the-home (FTTH) backhaul networks, RF sensitive areas (e.g. Hospitals), IT security applications, etc. [9].

SECTION II

RF VS. OPTICAL COMMUNICATION

One of the primary objectives we defined was to investigate into Optical Communications by comparing its standard to current market Radio Frequency (RF) communication standards. The RF spectrum is host to technologies such as Wi-Fi (802.11x), Ultra-Wideband (UWB), Bluetooth, etc. Since its bandwidth is limited to only 2.4 GHz in the RF Spectrum, it is subject to be highly congested, and exhibits a lower data rate capability. It addition, the restrictions within RF makes it expensive to license for commercial use. Optical communication on the other hand, is a license free spectrum with an almost unlimited data rate and is low cost for its development and installation. Key attributes specifically for Optical Wireless Communication (OWC) has its advantages over RF. The table below provides the main difference in terms of key parameters (Table 1).

Table 1.

Comparison of OWC and RF communication [9].

Characteristic	**OWC**	**RF**
Bandwidth	Not regulated	Licensed
Available line rates	< 10 Gb/s	< 1.25 Gb/s
Path losses	High	High
Multipath fading	No (large collector area)	Yes
Multipath distortion	Only in diffuse indoor systems	Yes
Noise sources	Ambient light	Interference from other users, electrical noise

Detection type	Incoherent	Coherent/Incoherent
Signal-to-Noise Ratio	Depends on optical signal power	Depends on RF signal amplitude
Receiver sensitivity	Low	High
Eye Safety	Required	N/A
Electromagnetic Compatibility	Yes	Conditional

OWC systems are already in development within the wireless world. The following figure below shows all the commercial RF and OWC technologies under standardization (Fig. 1).

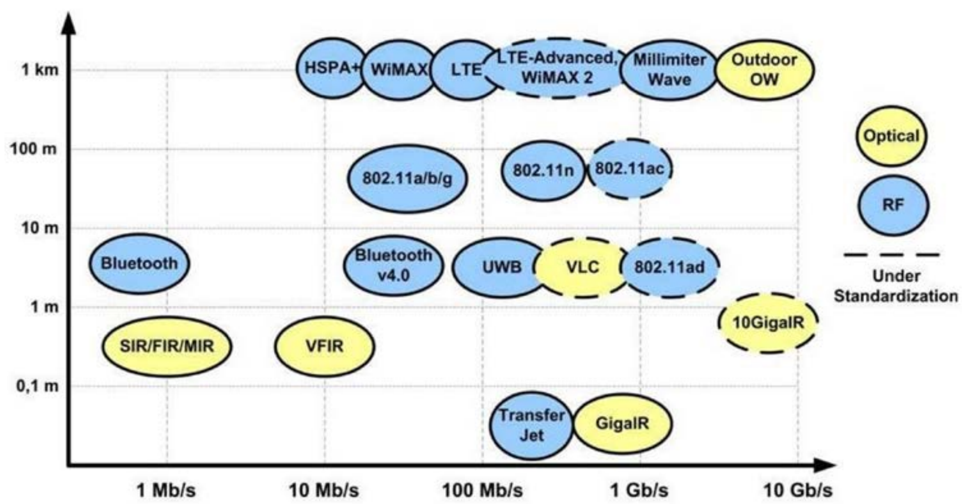

Fig. 1. Commercial RF and OWC technologies under standardization [8].

2.1. Electromagnetic Spectrum

When comparing Optical Communication to the RF Spectrum, it is important to note that over the span of the last 20 years, the RF spectrum has been proven to be vastly limited in meeting the needs for increasing data traffic. Next generation networks will need a greater bandwidth, and the visible light spectrum (VLS) includes hundreds of terahertz (THz) of license free bandwidth accessible for communication purposes. Seen below is the Electromagnetic spectrum (Fig. 2).

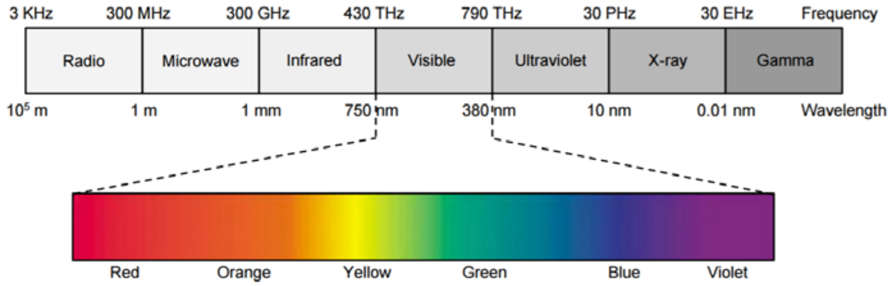

Fig. 2. The Electromagnetic Spectrum. VLS has Frequencies from 430 THz – 790 THz. [7].

2.2. Security Comparison

A key advantage that OWC possesses is a high level of transmission security. The narrow bandwidth is associated with a corresponding wavelength, preventing interception and effects of Electromagnetic Interference (EMI). Comparatively, RF transmission is readily subject to interception as a means of providing broadband access to a host of users [16]. In fact, RF systems like cellular networks, and wireless local area networks (WLAN) intentionally radiate the signals in all directions, thus, having no physical layer transmission security.

SECTION III

OPTICAL COMPONENT CHARACTERISTICS

For any reliable OWC system, the optical components that are utilized are crucial to determining its overall performance. Section 3 conveys the key characteristics of the optical components incorporated in the system, which are the optical light source (LED/LD), the optical detector, and the fiber optic cable.

3.1. Optical Light source

For OWC, the light source must have the appropriate wavelength (λ), numerical aperture (NA), high radiance with a small surface emitting area, long life, and a high modulation bandwidth (at 3-dB cutoff frequency) [10]. There exist different semiconductor devices that can be used, such as the Light Emitting Diode (LED), resonant-cavity LED, laser diode (LD), and vertical-cavity surface-emitting laser (VCSEL). The most commonly used and accessible are LEDs and laser diodes. In terms of determining if an LED or LD would be suitable for the design project, Table 2 seen below reveals a comprehensive comparison highlighting the key characteristics needed for a complete OWC system [14].

Table 2.

A comparison of LED to semiconductor laser diode (LD).

Characteristics	**LED**	**LD**
Optical output power	Low power	High power
Optical spectral width	25 – 100 nm	0.01 – 5 nm
Modulation bandwidth	~ 10 kHz – 100+ MHz	~10 kHz – 10+ GHz
E/O conversion efficiency	10-20%	30-70%
Eye Safety	Considered eye safe	Must be rendered eye safe
Directionality	Beam is broader and spreading.	Beam is directional and highly collimated.
Reliability	High	Moderate
Coherence	Non-coherent	Coherent
Drive and control circuitry	Simple to use and control	Threshold and temperature compensation circuitry.
Cost	Low	Moderate to High

These research findings supported the use of an LED as the preferred, and most cost effective option. Industrial Fiber Optics' IF-E99B is an edge emitting LED constructed out of a Gallium Aluminum Arsenide ($GaAlAs$) die that peaks its wavelength at 660 nm, emitting bright red. The LED itself is packaged with an internal micro-lens and held inside a precision molded housing which allows for easy, and efficient coupling of a plastic optical fiber (POF).

3.2. Optical detector

For optical detectors, the most commonly used are PIN Photodiodes, or Avalanche Photodiodes (APD). The component used for the optical detector was Industrial Fiber Optics' IF-D98 Photologic detector, a silicon (Si) PIN Photodiode with a spectral bandwidth between 400 to 1050 nm. For the incident wavelength of 660 nm, the responsivity was measured to be ~ $0.4*10^{-6}$ A/W. The Photodetector is a key component in an OWC system because it directly affects the initial bandwidth at which the RX circuit can operate from the transmitted optical power. The theoretical bandwidth is determined from the 3-dB electrical bandwidth $\boldsymbol{f_{3-dB}}$ as:

$$f_{3-dB} = \frac{0.35}{t_r} \quad \text{[Eq. 1]}$$

The IF-D98's photodiode has a rise time $(\boldsymbol{t_r})$ of 3.0 ns; therefore, its theoretical bandwidth capacity is 116.33 MHz.

3.3. Plastic Optical Fiber

The Plastic Optical Fiber (POF) is based on a Poly-Methyl-Methacrylate (PMMA) compound material with a step index profile and 1mm core diameter. The large core diameter (~ 0.98 mm) allows for easy installation, and is not likely to suffer damage from adding any sort of connectors. The ideal optical sources for POF are within the visible light spectrum (VLS). Table 3 shows the comparison on the following optical sources when utilized for POF coupling, with an emphasis focused specifically on LEDs and LDs.

Table 3.

Light Sources for PMMA Plastic Optical Fibers [14].

Parameter	**LED**	**LD**	**VCSEL**	**RC-LED**
Wavelength (nm)	520,570,650	650,520,488	660	650
Threshold current	None	> 15 mA	20 mA	None
Optical power (mW)	2	Up to 20	1	2
Data rate	250 Mbps	2 Gbps	5 Gbps	500 Gbps
Optical power sensitivity to temperature (dB/C)	-0.01,-0.05,-0.01	- 0.02	-0.08	-0.03
Wavelength sensitivity to temperature (nm/C)	0.04,0.12,0.12	0.18	0.06	0.07
Spectral Bandwidth (nm)	40,25,30	2	1	10
Cost	Very cheap	650 nm is cheap; others are expensive	Expensive	Cheap
Operating Temperature (C)	85	85	50	85

POFs have been optimal with use for a wavelength at 650-660 nm, as seen with the following characteristics when considering cost, simplicity, and eye safety [10].

SECTION IV

COMMUNICATION SYSTEM OVERVIEW

Section 4 provides the key overview of the communication system with each subsection highlighting its functionality in terms of the complete system design. As previously expressed from the characteristics of the optical components, the additional circuitry ultimately determines how the complete communication system will perform throughout the process of data transmission.

4.1. Optical Data Link Design

The following OWC system addresses the key aforementioned parameters and mitigates foreseen challenges discovered by the limited data rate from the Fib-Opt click boards and additional simulation results from the optical system simulation.

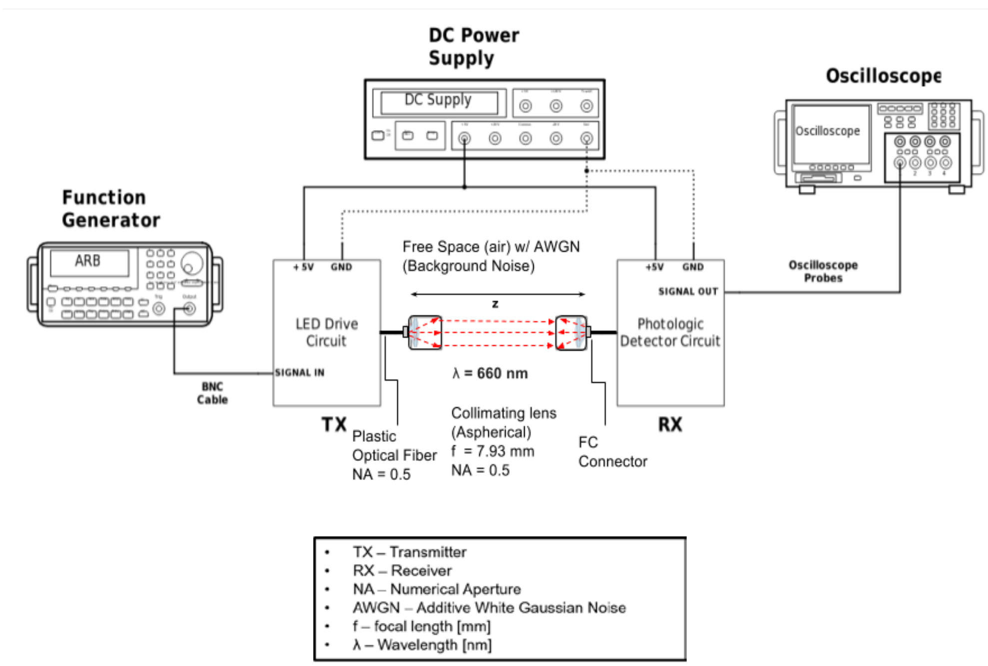

Fig. 3. Diagram and notation of optical communication system.

This setup has been commonly established for an accurate Intensity Modulation/ Direct Detection (IM/DD) Line-of-sight (LOS) data link. The function generator is also called an Arbitrary Waveform Generator (AWG). The AWG is capable of providing an AC coupled logic data input, which is sufficient to apply On-off Keying (OOK) modulation in a Non Return-to-Zero (NRZ) format for testing the system. The bandwidth requirement has been set to be slightly higher than the frequency limit of the AWG, which is 60 MHz. A higher bandwidth requirement ensures the system has the capacity to be test how high speed the data rate can be achieved accurately [6]. Due to the simplicity of Industrial Fiber optics installation, the following LED and PD are both products from the same manufacturer. Seen in the table below are their key characteristics (Table 4).

Table 4.

Comprehesive list of key specifications for (a) IF-E99B and (b) IF-D98

IF E99B	
Peak Wavelength	650 nm
Output power coupled into Plastic Fiber.	630 μW -2 dBm
Switching times (R_l = 47 Ω, If = 10 mA)	3 ns
Cut off Frequency	70 MHz
Data Rate	156 Mbps

IF D98	
Spectral Bandwidth	400 – 1050 nm
Light required to Trigger **(λ = 660 nm, V_cc = 5V)**	6.3 μW - 22 dBm
Output Switching times	3 ns
Data Rate	4 - 156 Mbps

4.1.1. B.O.M. and cost comparison analysis

The bill of materials used for the complete OWC system shows all the components for each respective circuit along with the optical components. The total cost for development is $279.07 not accounting for prices of wires, and other tools used to accomplish the design, such as lab equipment (function generator, DC power supply, Oscilloscope) and the fiber cutting tool. The original experimental set-up featured two Fiber Opt click boards and two Raspberry Pi 3 single board computers. If the same free space optical setup was used with the Fiber Opt click boards, the price would total to $296.45. Furthermore, our design can have one Raspberry Pi 3 while the Fiber opt click boards would need two, totaling to $319.02 and $336.40 respectively. In conclusion, not only is our design a cost effective solution compared to a market product, it is capable of transmitting information at a much faster data rate, up to 156 Mbps compared to 512 Kbps.

IF-E99 LED	$37.50
2 Input AND gate	$0.49
2 pole input screw terminal (2)	$1.98
4 pole input screw terminal	$2.11
0.1 μF capacitor (ceramic)	$0.10
4.7 μF capacitor (electrolytic)	$0.10
100 Ω resistor (0.25 W)	$0.78
51 Ω resistor (0.25 W)	$0.60
51 Ω resistor (0.25 W)	$0.60
SpeedyProto PCB Protoboard	$2.00
FC240FC-B FC/PC Fiber collimator package (2)	$159
FC/FC commercial grade POF patch cord (1.0 m)	$29.50
IF-D98 Photologic detector	$31.00
MC100ELT2100DGOS-ND (PECL-to-TTL translator)	$3.98
Sparkfun SOIC-to-DIP Adapter	$2.95
511 Ω resitor (0.25 W)	$0.72
0.1 μF capacitor (ceramic)	$0.10
2 pole input screw terminal (2)	$0.99
4 pole input screw terminal	$2.11
10 μF capacitor (electrolytic)	$0.47
SpeedyProto PCB Protoboard	$2.00

Fig. 4. Bill of materials for OWC system (Green – TX, Grey – Free space channel, Blue – RX).

4.2. Transmitter (TX) characterization

The TX circuit's main function is to drive current through the LED. The circuit utilized for the fiber optic LED is a simple setup that allows the AWG to be connected as an input signal. We first establish our initial circuit for testing purposes, and then incorporate a more robust design for further use in the experimental testbed.

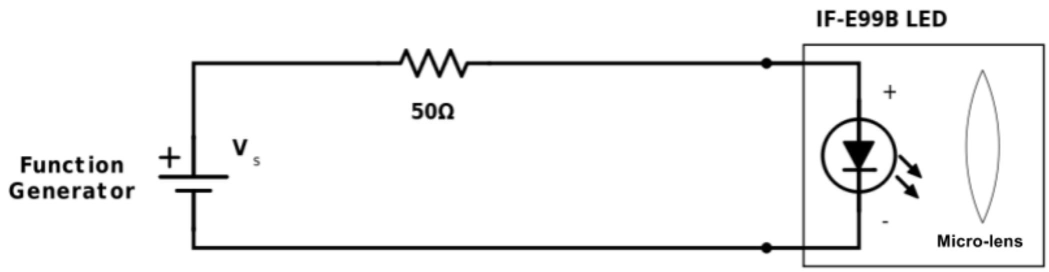

Fig. 4. Initial Transmitter circuit (TX #1).

The initial TX circuit chosen directly connects the function generator to the IF-E99B LED. The function generator controls the source of light (LED) by varying the current flow across the LED's PN junction. The function generator itself is a source of periodic, square waves of voltage, or AC waveforms (i.e. Sine, etc.). The function generator uses its internal resistance to limit the current through the LED via a 50 Ω BNC cable. Even though we are able to vary the current, the function generator is not an ideal voltage source [1], thus, we develop a comprehensive circuit design in order to move forward with the TX circuit within the system.

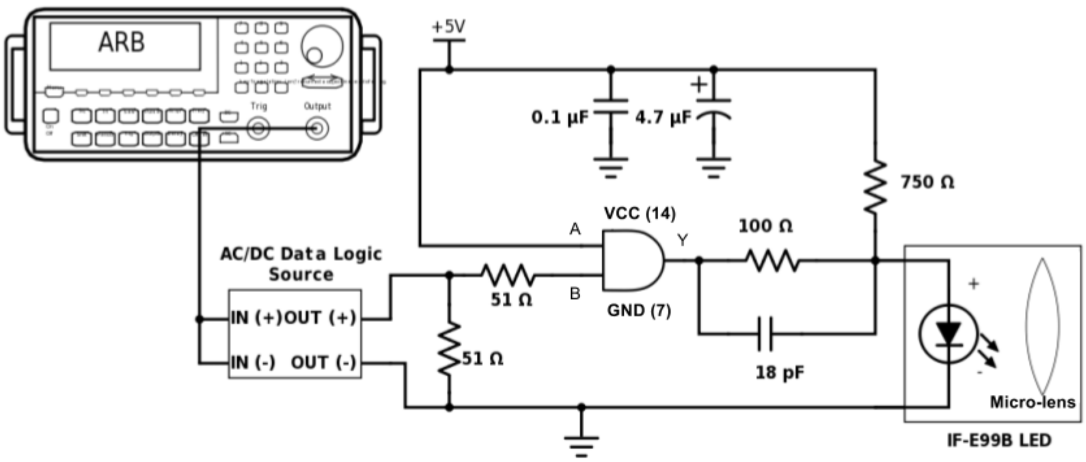

Fig. 5. Final Transmitter circuit (TX #2).

The final design for the transmitter (TX) highlights the recommended use of driving the IF-E99B LED. The schematic diagram is pictured above. The function generator provides AC/DC logic data to the 2-input AND gate integrated circuit (IC) that also couples a constant DC logic of +5V to supply current through the LED. The 0.1 μF and 4.7 μF capacitors are bypass capacitors close to VCC to prevent voltage swing or noise caused by the AC component.

4.3. Receiver (RX) characterization

The primary role that the receiver circuit serves is for post processing of the carrier signal from the photodiode and demodulating the data. IF-D98 is a photo logic detector comprised of a PIN photodiode, linear amplifier and a Schmitt trigger. Its recommended circuit is described below that converts electrical PECL inputs to TTL level outputs.

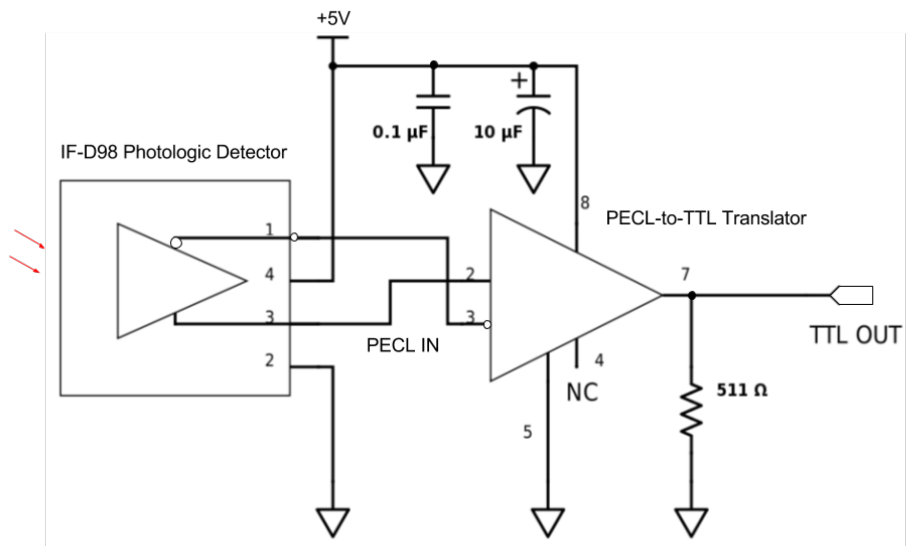

Fig. 6. Final Receiver circuit (RX).

The operation of the IF-D98 Photologic detector is established as stages responsible for optical to electrical conversion (Fig. 7). The internal micro-lens will focus the incoming light onto the photodiode. The photodiode is a reversed biased semiconductor device responsive to high-energy photons. Photodiodes operate by absorption of photons or charged particles and generate a flow of current in an external circuit, proportional to the incident power. The linear amplifier is an electronic circuit whose output is proportional to its input, but is capable of delivering more power into a load, thus, the Schmitt Trigger in this case. The Schmitt Trigger is a comparator circuit that is implemented by applying positive feedback to the non-inverting input of the linear amplifier. Additionally, it functions as an active circuit that converts an analog input signal to a digital signal. Lastly, the PECL logic compatible totem pole output completes the conversion. Emitter-coupled logic (ECL) is the fastest logic circuit family available for conventional logic-system design. High speed is achieved by operating all bipolar transistors out of saturation, thus avoiding storage-time delays, and by keeping the logic signal swings low (~0.8 V or less), thus reducing the time required to charge and discharge the various load and parasitic capacitances. Saturation in ECL is avoided by using the BJT differential pair as a current switch. Positive emitter-coupled logic is a further development of ECL using a positive 5 V supply instead of a negative 5.2 V supply, thus enabling more compatibility with common power supply levels.

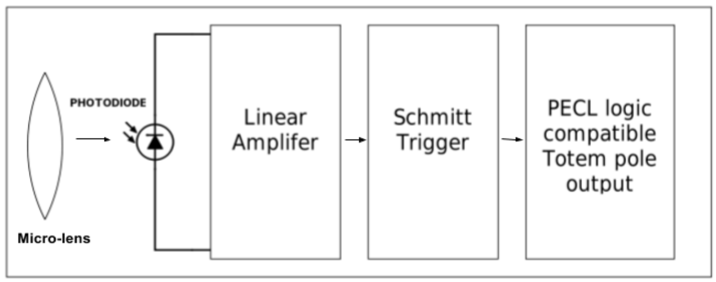

Fig. 7. IF-D98 Photologic detector characteristics.

The MC100ELT21 (Fig. 8) is a device called a differential PECL to TTL translator. Because PECL levels are used, only VCC (+5 V) and GND is required. The key features are a typical propagation delay of 3.5 ns, and translation from PECL inputs to CMOS/TTL outputs.

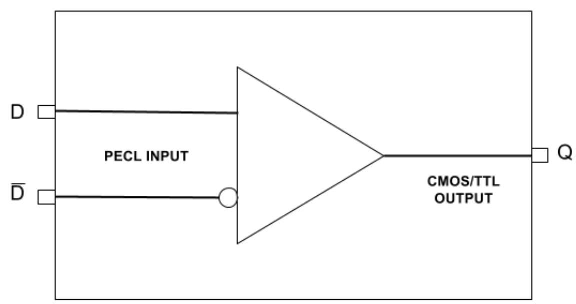

Fig. 8. PECL-to-TTL translator diagram (MC100ELT21).

4.4. Free Space Channel characterization

In order to focus the light across free space, we compared using a collimating lens or objective lens to achieve successful beam expansion. Additional research revealed that a lens capable of collimating the light with little to no spherical aberration of light rays is an aspherical lens. The aspherical lens is preferred over the objective lens because the magnification (10x) produces an airy disk, and its NA is 0.25, a mismatch to the POF NA of 0.5. The loss of light rays carrying data would be a significant penalty. The FC240FC-B FC/PC Fiber collimator package is pre-aligned to collimate light from an FC-terminated fiber and has no movable parts making for compact and easy integration into our experimental setup. The fiber collimator package couples the POF to both the IF-E99B LED and IF-D98 Photologic detector at both ends of the communication system.

Fig. 9. Thorlabs F240FC-B FC/PC Fiber Collimation package.

Seen below shows the interaction of light rays as they will occur throughout the system (Fig. 10). The LED will emit the wavelength through the fiber which will bend the light at different angles leading to a phenomenon known as modal dispersion. After light propagates through the fiber, the aspherical lens will bend the light to be parallel and expand the beam across free space over a variable distance from the transmitter and receiver.

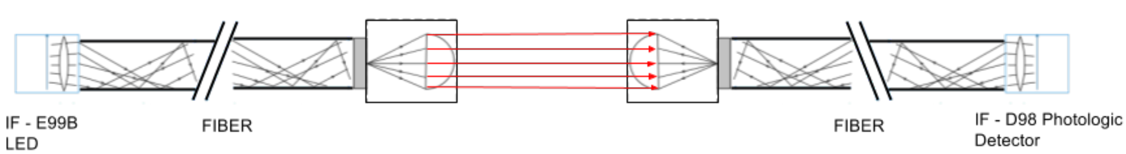

Fig. 10. Interaction of light rays throughout the system [14].

4.4.1. Why use high NA collimators?

The purpose of using a high NA collimator affects the incident beam of light that will propagate through free space [4]. Light emitted from an LED through a multimode fiber produces a wide cone of light, which can be calculated from the relationship stated below where Eq. 2 is the Numerical Aperture.

$$NA = sin(\frac{\theta_{max}}{2}) \quad \text{[Eq. 2]}$$

$\boldsymbol{\theta_{max}}$ is the divergence angle that is dictated by the reflection between the fiber's core and cladding (Fig. 11). In the case of multimode fibers and its NA value, we can conclude that the light is emitted at an angle of 60 °.

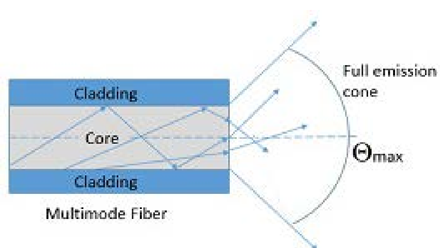

Fig. 11. Optical fiber emission of light [2].

We mitigated this result by coupling the high NA fiber to a high NA collimator. The result produced good power throughput of the light through the lens, and also captures majority of the light rays that will be collimated. Seen below indicates the difference of interaction if a low NA lens is used or one that is the same NA or slightly higher for coupling with the high NA fiber (Fig. 12).

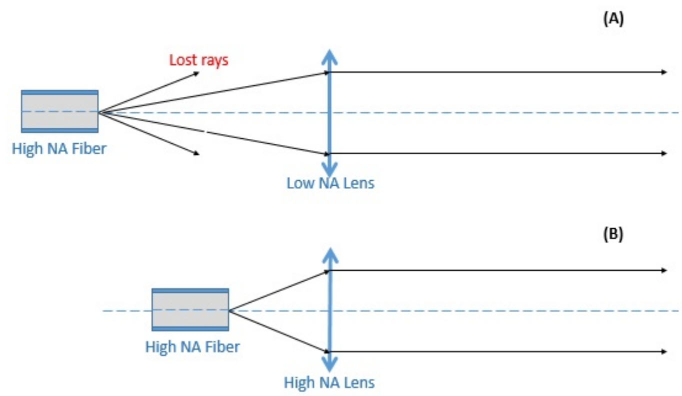

Fig. 12. (A) High NA fiber - Low NA lens pair, (B) High NA fiber - High NA lens pair [2].

4.4.2. Beam quality and beam properties

In order to understand key aspects of the beam across free space, we address the question of the beam quality of the light coming out of the fiber. We calculated the maximum M^2 factor of the input light with the following equation and parameters (Eq. 3).

$$M^2_{max} = \frac{\pi r_{core} NA}{\lambda} = \frac{(\pi)(490\mu m)(0.5)}{660nm} = 1166.197 \quad \text{[Eq. 3]}$$

Even though we could not determine the details of the beam intensity profile with the M^2 factor alone, we can assume that the optical power is well spread over all the guided modes in the POF [3].

The light source is confined to a narrow cone as mentioned before. As the beam propagates outward, it slowly diverges or fans out. For an electromagnetic beam, beam divergence is the angular measure of the increase in the radius or diameter. Even though a beam retains its Gaussian profile for a specific distance, the optical output power determines how far the distance can be without diverging. For this reason, the diagram seen below explains why the high NA collimator is used compared to a low NA collimator that would have caused beam divergence (Fig. 13). For our setup, we calculate the beam diameter of the light (Eq. 4).

$$d_{large} = \frac{7.93mm}{0.5} = 15.86mm \quad \text{[Eq. 4]}$$

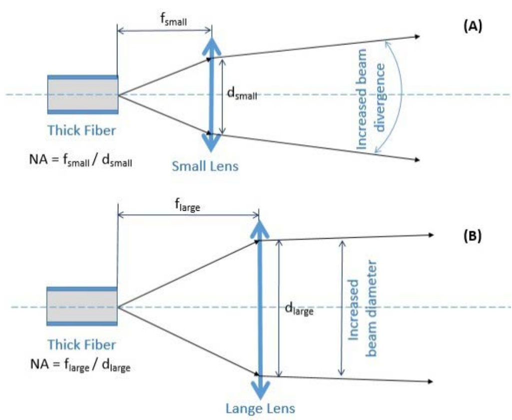

Fig. 13. Comparison of beam diameter between high NA lens and low NA lens [2].

4.5. Modulation Scheme characteristics

The modulation scheme applied to test our system is digital pulse code modulation (PCM), which is also referred to as OOK modulation [12]. Both Non-return-to-zero (NRZ) and Return-to-zero (RZ) coding can be implemented via the Function generator. Further testing for the Bit Error Rate (BER) can be used for this modulation scheme, and additional supplemental experiments as well, which provides a sufficient means of testing the OWC system.

SECTION V

SIMULATIONS AND EXPERIMENTAL RESULTS

Section V covers key simulation and experimental results directly addressing the tasks of defining requirements and design for a reliable, proof-of-concept OWC system. The goals and motivation is to determine the best way to achieve secure transmission over a variable distance between the transmitter (TX) and receiver (RX) circuits.

5.1. POF Frequency Response and Bandwidth

A POF typically supports thousands of different optical modes, and each individual optical mode has a particular frequency and speed at which data propagates. Due to the differences in propagation speed, the data signal gets increasingly distorted as it travels down the fiber. If adjacent digital pulses overlap, the receiver might not be able to decode the data [8]. This phenomenon is known as modal dispersion. The bandwidth is dependent on the modal dispersion. It is the parameter that determines the maximum bandwidth transmitted through the fiber.

Changing the POF length has two effects on the frequency response. Firstly, the bandwidth is decreased by increasing the POF length. Secondly, the roll-off is increased by increasing the POF length. For POF's less than 20m, the frequency roll-off is smaller than 4.2 dB per octave [14]. Using a binary signal is better than any other modulation scheme for these lengths, which is sufficient evidence to apply On-Off Keying (OOK) modulation in terms of accomplishing design objectives.

Shannon's Capacity formula relates the maximum achievable capacity (transmission bit rate) over a given channel for signal and noise characteristics and bandwidth. Below, C is the max capacity of the channel, and B is the bandwidth (Eq. 5).

$$C = B \cdot log_2\,(1 + \frac{S}{N}) \quad \text{[Eq. 5]}$$

Due to the roll-off of the system (POF and optical receiver), Shannon's Capacity has been reported to state that data rates ranging from 4000 Mbps to 1500 Mbps is achievable for POF lengths from 20 – 40 m when using a binary signal technique.

5.2. P-I relationship for optical source and modulation response

Determining the output optical power of the LED provides essential understanding of the effectiveness of the TX circuit, which also affects the total system performance [13]. The LED optical power output produced a linear relationship by changing the injection current when using the setup of TX circuit #1 (Fig. 4). The plot seen below was generated via MATLAB® (Fig. 14).

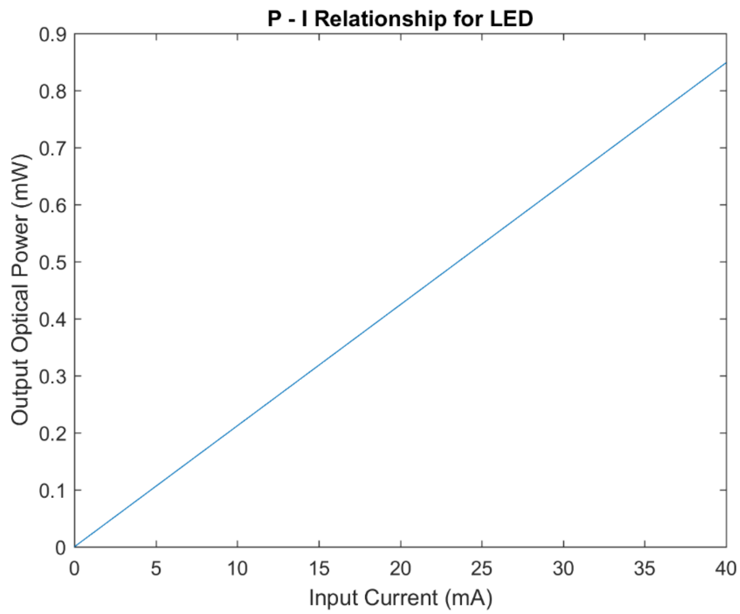

Fig. 14. Input current vs Output optical power plot for IF-E99B LED.

The modulation response for the LED was determined by calculating the electrical bandwidth(f_{3dB}) which equates the two equations seen below. The recombination lifetime for the LED is denoted as τ and t_r is denoted as the rise time [15].

$$f_{3dB} = \frac{1}{2\pi\tau} = \frac{0.35}{t_r} \quad \text{[Eq. 6]}$$

The calculated rise time (t_r) is 3 ns, establishing the 3 dB electrical bandwidth of the LED at 116 MHz. As a result of the recombination lifetime (τ) throughout the process, it produces a delay to the waveform of the output optical power for an input square wave signal generating high-low levels of input current (Fig. 15).

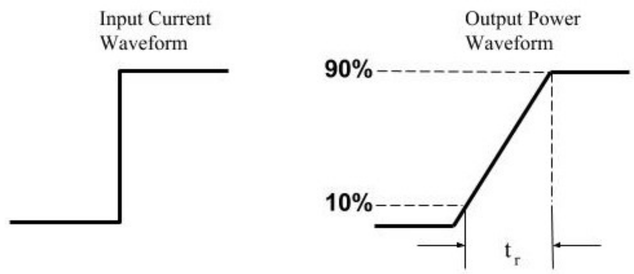

Fig. 15. Rise time of the optic source (LED) [15].

5.3. LOS propagation model

This simulation was modeled in MATLAB® in order to further understand the free space channel characteristics. For an indoor OWC system, configuration is dependent on the following parameters: degree of directionality of a transmitter and receiver, and the existence of the Line of Sight (LOS) between TX and RX. Intensity modulation with direct detection (IM/DD) is the de-facto method for implementing optical wireless systems principally due to its low cost and complexity of setup [11]. The following equations were used to model the LOS channel gain across an indoor free space channel.

$$P_{los} = P_t \cdot \frac{(m+1)}{2\pi d^2} \cdot cos^m(\phi) \cdot T_s(\psi) \cdot g(\psi) \cdot cos(\psi), 0 \leq \psi \leq \Psi \quad \text{[Eq. 7]}$$

$$m_1 = \frac{-\ln 2}{\ln(\cos \Phi_{1/2})} \quad \text{[Eq. 8]}$$

Eq. 7 is the Received optical power for the line of sight (P_{los}). P_t is the transmitted power from an LED, ϕ is the angle of irradiance with respect to the transmitter axis, d is the distance between an LED and the detector's surface. $T_s(\psi)$ is the filter transmission, $g(\psi)$ is the concentrator gain, and both are normalized to 1 for simplicity of calculation and the physical setup. Ψ is the concentrator field of view (FOV). Eq. 8 is the Semi-angle m is the order of Lambertian emission, and is given by the transmitter half angle (at half power). For our calculations, m = 1 and $\Psi_{1/2}$= 60°. The MATLAB program allowed us to choose a variable distance (d) and determine the calculated received power for free space propagation [11].

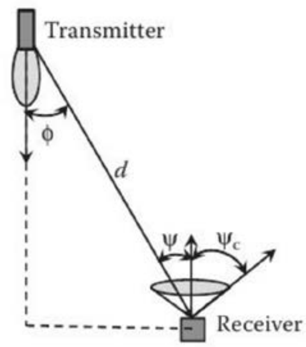

Fig. 16. LOS Propagation model diagram [11].

5.4. Power budget analysis

This experiment accounts for the physical boundaries of our OWC system that contribute to the total power budget for the system. Fig. 17 reveals that the fiber and connectors attribute to power loss in decibels (dB).

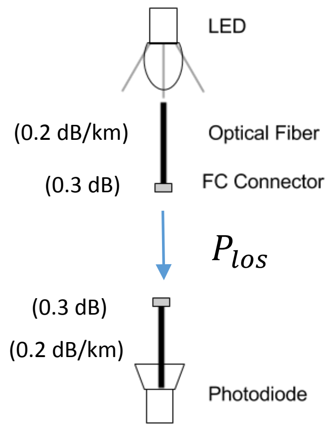

Fig. 17. Modified power budget analysis from LOS propagation model.

Whenever the distance would be changed, P_{los} would become the variable with the following values from the POF and FC connectors being fixed for both the TX and RX in the OWC system. For a more thorough analysis, we account for the LED-to-air transmission loss before propagation through the POF, expressed in Fig. 18. The boundary is the physical medium where n_1 is the refractive index of the LED material (AlGaAs) is determined to be 3.8177. The refractive index n_2 is air, which is 1.

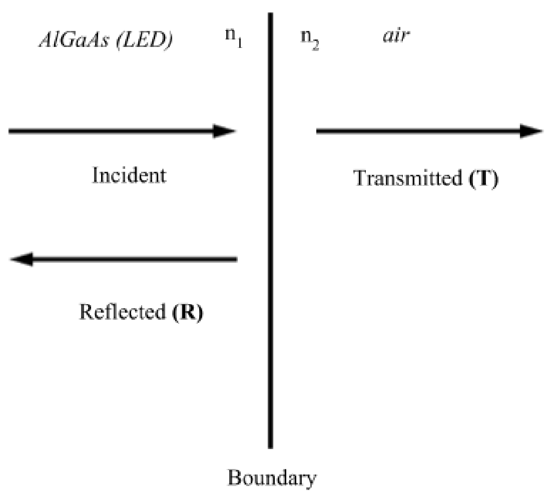

Fig. 18. LED material to air reflectance and transmission [15].

We determine the calculations from the following equations seen below. R is the reflection at the boundary, T is the transmission, and Power transmission loss is expressed in Eq. 11. P_{RX} is the total received power from the calculated P_{los} with P_{loss} being the total from the POF, FC connector, and the LED-to-air power transmission loss combined. We calculate the P_{loss} = 2.418 dBm. We then can convert the units from dBm to mW using Eq. 13.

$$R = (\frac{n_1 - n_2}{n_1 + n_2})^2 \text{ [Eq. 9]}$$

$$T = 1 - R \text{ [Eq. 10]}$$

$$P_{dBm} = -10 \cdot log_{10}T \text{ [Eq. 11]}$$

$$P_{RX} = P_{los} - P_{loss} \text{ [Eq. 12]}$$

$$P_{mW} = 1mW \cdot 10^{\frac{P_{dBm}}{10}} \text{ [Eq. 13]}$$

SECTION VI

CONCLUSION AND FUTURE IMPLICATIONS

In conclusion, we are able to calculate the total rise time for the system, seen expressed with Eq. 18. With the rise time at 3.35 ns, we determined with the electrical bandwidth equation, f_{3dB} (Eq. 1) that for a digital encoded signal, the maximum theoretical data rate is $2 \cdot Bandwidth\ (f_{3dB}) = 165\ Mbps$.

$$t_{r(system)} = \sqrt{(t_r{}^2(TX) + t_r{}^2(RX))} = 3.35ns \quad \text{[Eq. 14]}$$

In order to further understand our communication system, we imply that the signal-to-noise ratio (SNR) will gradually increase as the propagation distance would increase between the TX and RX circuits. Future experiments are described below to develop a more comprehensive analysis of the communication system's real time performance.

6.1. BER vs. free space distance

This experiment will begin by having both lenses next to each other and then begin separating the distance between them by centimeters [5]. Data measurements will be made and the Bit Error Rate (BER) analyzed at each corresponding distance will be recorded until the free space distance will result in an undesirable BER threshold.

From this setup, we can then monitor the signal integrity from the TX circuit to the RX circuit over free space. The Oscilloscope would be connected to the input data signal and the output signal to show the waveforms rise-fall times over the course of data transmission.

6.2. Recommendation for future designs

Possible additions and ways to improve the communication system could be to place both the TX and RX circuit on a single Printed Circuit Board (PCB). Even though it may add to the total cost of materials, two boards will create a free space optical transceiver giving a user full duplex communication capability. Any other modifications can apply to either the TX circuit design or the RX circuit design in order to meet the user's specific needs. Orientation and alignment can be altered with different configurations, but will need to remain as a LOS link for successful transmission of data.

REFERENCES

[1] "ELEC 242 Lab - Experiment 1.2," in "ece.rice.edu," 2012 2012.

[2] "FCM Collimators for High NA Fibers," in *FCM Collimators for High NA Fibers*, ed: Prizmatix, 2015.

[3] R. Paschotta. (2013). *Beam Quality Limit for Multimode Fibers*.

[4] Y. Chen, S. Wen, Y. Wu, Y. Ren, W. Guan, and Y. Zhou, "Long-range visible light communication system based on LED collimating lens," *Optics Communications*, vol. 377, pp. 83-88, 10/15/ 2016.

[5] P. Shamsudheen, E. Sureshkumar, and J. Chunkath, "Performance Analysis of Visible Light Communication System for Free Space Optical Communication Link," *Procedia Technology*, vol. 24, pp. 827-833, // 2016.

[6] T. Kishi, H. Tanaka, Y. Umeda, and O. Takyu, "A High-Speed LED Driver That Sweeps Out the Remaining Carriers for Visible Light Communications," *Journal of Lightwave Technology*, vol. 32, no. 2, pp. 239-249, 2014.

[7] P. H. Pathak, X. Feng, P. Hu, and P. Mohapatra, "Visible Light Communication, Networking, and Sensing: A Survey, Potential and Challenges," *IEEE Communications Surveys & Tutorials*, vol. 17, no. 4, pp. 2047-2077, 2015.

[8] D. K. Borah, A. C. Boucouvalas, C. C. Davis, S. Hranilovic, and K. Yiannopoulos, "A review of communication-oriented optical wireless systems," *EURASIP Journal on Wireless Communications and Networking*, vol. 2012, no. 1, p. 91, 2012// 2012.

[9] Z. Ghassemlooy, W. Popoola, and S. Rajbhandari, "Introduction," in *Optical Wireless Communications: System and Channel Modelling with MATLAB®*: CRC Press, 2012, pp. 1-33.

[10] Z. Ghassemlooy, W. Popoola, and S. Rajbhandari, "Optical Sources and Detectors," in *Optical Wireless Communications: System and Channel Modelling with MATLAB®*: CRC Press, 2012, pp. 35-75.

[11] Z. Ghassemlooy, W. Popoola, and S. Rajbhandari, "Channel Modelling," in *Optical Wireless Communications: System and Channel Modelling with MATLAB®*: CRC Press, 2012, pp. 77-159.

[12] Z. Ghassemlooy, W. Popoola, and S. Rajbhandari, "Modulation Techniques," in *Optical Wireless Communications: System and Channel Modelling with MATLAB®*: CRC Press, 2012, pp. 161-265.

[13] Z. Ghassemlooy, W. Popoola, and S. Rajbhandari, "System Performance Analysis," in *Optical Wireless Communications: System and Channel Modelling with MATLAB®*: CRC Press, 2012, pp. 267-346.

[14] M. Atef and H. Zimmermann, *Optical Communication over Plastic Optical Fibers Integrated Optical Receiver Technology*. Berlin, Heidelberg: Springer Berlin Heidelberg : Imprint: Springer, 2013.

[15] J. C. Palais, *Fiber Optic Communications*. Upper Sadle River, New Jersey: Pearson Education, 2005.

[16] R. Carlson, "Wireless Transmission Security using SONAbeam Free-Space Optical Communcations," 2013, Available: http://www.fsona.com/tech/white_papers/WHTPAP-Wireless_Security.pdf, Accessed on: 10/06/2016.